Dynamic Modelling of a Two-stage Helical Gearbox with the Consideration of Nonlinear Rolling Bearing Contact and Time-varying Meshing Stiffness

Ganghui Xu, Xin Xiong*, Xiuting Yan, Chen Shen
School of Mechatronic Engineering and Automation
Shanghai University
Shanghai, China
E-mail: xxiong@shu.edu.cn

***Abstract*—Gearbox system is a vital part in the industry and our daily lives, of which the dynamic behavior is important for equipment's prognostics and health management. In this paper, considering the effects of time-varying stiffness and nonlinear characteristics of bearings, one dynamic model of a two-stage gearbox test rig with helical gears is established, in which the motion of housing is included. An efficient expression of time-varying meshing stiffness has been adopted to study the gear dynamics, with the model of helical gear pair derived from the one of spur gear pair. Based on the coupling gear-rotor-bearing dynamic model, steady-state vibration response of the gearbox has been obtained by using numerical methods, and the vibrations of the input and output positions are compared and analyzed. The results prove that the position where the sensor is placed has an effect on the signal detection, and the effect of time-varying meshing stiffness on system response is discussed.**

Keywords-two-stage gearbox; vibration response; helical gears; housing; time-varying stiffness

I. INTRODUCTION

Gearbox is among the most important mechanisms for transmission of motion and power in numerous industrial applications and our daily lives. Because of their growing use in modern technology, gearbox health monitoring and early fault detection have become the subject of intensive investigation and research [1,2]. Although vibration signals are often used in condition monitoring and fault diagnosis of gearboxes, measured signals are generally affected by the complicated coupling of the system and the transfer path between the excitation source and measurement sites. Thus, vibration simulation of gear transmission system is of great significance to study the characteristics of vibration signals and the damage dynamics, which can provide theoretical supports for running state identification of gearbox systems [3].

A great many researches have been conducted to study the dynamic modelling of gear-meshing operation over the past several decades, e.g., from the simplest mass-spring single degree-of-freedom models to the complicated multiple degree-of-freedom dynamic models considering various internal and external excitations [4]. In general, the nonlinear dynamic behaviors of gear transmission are governed by the time varying stiffness, static transmission error, backlash and sliding friction.

Above them, the time-varying meshing stiffness is one principal issue in gear nonlinear dynamics, which is due to the change of the number of conjugate tooth pairs in contact during the convolute action [5]. Therefore, the calculation of varying stiffness has become a hotspot among the research works. Common methods include analytical method, finite element (FE) method, and analytical-FE method. Generally, FE method is time-consuming, while analytical methods show good results with less computation time, as many studies have shown [6]. Common analytical methods mainly include empirical formula method, deformation method, harmonic balance method and potential energy method. The ISO standard 6336-1-2006 is typical representative of empirical formula which defines a method to calculate the mesh stiffness, but it can only calculate average mesh stiffness. A so-called potential energy method was presented by Yang and Lin [7] which can calculate the time varying stiffness accurately and has been improved by several later researchers [3,8,9], but the proposed method is still not convenient enough to utilize in the modelling of gearbox system.

Furthermore, support bearings and shafts also make significant contributions to the gearbox vibration. In most previous studies, bearings in the gearbox tend to be simplified to linear support models which neglect their nonlinear characteristics, while shafts are usually assumed as rigid [10].

In this contribution, a coupled gearbox dynamic model is established to simulate the vibration response of a two-stage gearbox test rig with helical gears. Nonlinear contact mechanism is considered in the model of rolling bearing, and an efficient method is adopted to express the time-varying meshing stiffness of each gear pair. Finally, vibrations of the gearbox housing are simulated at the input and output positions of the gearbox, which are further analyzed in the time and frequency domain.

II. GEAR PAIR DYNAMICS

A. Time-varying Stiffness Representation

Generally, excitations of the gear system can be divided into two categories, i.e., the internal and the external excitation. In our study, the gear mesh is assumed to be free from contact loss as gear pairs always work under enough loads. Hence, only the meshing stiffness and the external torque are taken into consideration. As is known, the contact ratio of a helical gear

978-1-7281-0860-5/19/$31.00 ©2019 IEEE

pair (ε_α) is mostly not an integer which means the number of the tooth pairs in mesh changes periodically. While the stiffnesses of tooth pairs are the sum of the stiffness of each tooth pair in mesh, the total stiffness of a helical gear pair also varies periodically as the gear operates. In this paper, the total number of tooth pairs in contact fluctuates between n and $n+1$, which is characterized by the contact ratio ε_α ($n \le \varepsilon_\alpha < n+1$).

The spur gear undergoes sudden changes in total stiffness during the alternate mesh of the single and double tooth pairs. But for the helical gear, as the changing mode of meshing line is 'point-line-point', the stiffness will not change abruptly, but still having evident periodic fluctuations. The model of Wang [11] has been adopted in this study to fit the time-varying meshing stiffness, which can be expressed by (1-2).

$$k_m(t) = k_0 + \sum_{i=1}^{3} k_i \cos(i f_m t + \varphi_i) \tag{1}$$

$$\begin{cases} k_0 = (0.75\varepsilon_\alpha + 0.25) k_{th} \\ k_i = \dfrac{\sqrt{2 - 2\cos[2\pi i(\varepsilon_\alpha - n)]}}{\pi i} k_{th} \\ \varphi_i = \arctan \dfrac{1 - \cos[2\pi i(\varepsilon_\alpha - n)]}{\sin[2\pi i(\varepsilon_\alpha - n)]} \end{cases} \tag{2}$$

where $k_m(t)$ is the total time-varying stiffness of a helical gear pair and f_m represents meshing frequency of this gear pair. k_{th} is the stiffness of an individual tooth pair in contact which can be calculated through the ISO standard 6336-1-2006. k_0 is the average mesh stiffness value while k_i and φ_i are the i^{th} Fourier coefficient and phase angle of $k_m(t)$, respectively.

B. Spur Gear Pair Modelling

The meshing model of the spur gear pair is usually simplified to a spring damping system [10], as shown in Fig. 1. It includes a pair of cylindrical masses connected along the line of action by a position-dependent stiffness $k_m(t)$, a damping coefficient c_m and a combined effect of transmission error excitation $e(t)$.

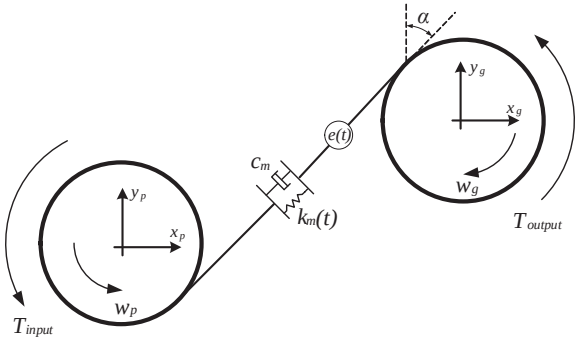

Figure 1. The spur gear pair model.

The degrees of freedom contained in the above model are two rotational (θ_p, θ_g) and four translational (x_p, y_p, x_g, y_g), from which the equations of meshing force are deduced by (3-4).

$$F_m = k_m(t) \bullet \delta_{spur}(t) + c_m \bullet \dot{\delta}_{spur}(t) \tag{3}$$

$$\delta_{spur}(t) = (x_p - x_g) \bullet \sin\alpha + (y_p - y_g + r_p\theta_p - r_g\theta_g) \bullet \cos\alpha \tag{4}$$

where F_m is the meshing force along the line of action which can be orthogonally decomposed into horizontal and vertical directions, $\delta_{spur}(t)$ is relative displacement between the gears along the line of action, $x_p, y_p, \theta_p, r_p, x_g, y_g, \theta_g, r_g$ represent translational or rotational motion and radius of the driving gear and the driven gear respectively. α is pressure angle. c_m is the mesh damping coefficient which is usually calculated by the empirical formula shown in (5) where ξ is damping ratio of which the value ranges generally from 0.03 to 0.17.

$$c_m = 2\xi \sqrt{\frac{k_0 r_p r_g I_p I_g}{r_p^2 I_p + r_g^2 I_g}} \tag{5}$$

C. Helical Gear Pair Modelling

Due to the existence of the helix angle β, the helical gear pair will generate an axial component during the meshing process, as shown in Fig. 2. In this study, the meshing model of the helical gear pair is derived from the one of spur gear pair, which is essentially consistent with the expression in other literature [12] after some formula derivation.

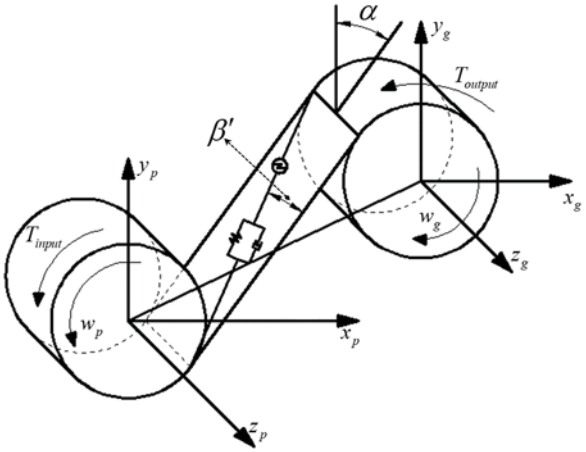

Figure 2. The helical gear pair model.

The meshing force expressions of the helical gear pair are formulated by (6-7).

$$F_m = k_m(t) \bullet \delta_{helical}(t) + c_m \bullet \dot{\delta}_{helical}(t) \tag{6}$$

$$\delta_{helical}(t) = \delta_{spur}(t) / \cos\beta' \tag{7}$$

where $\delta_{helical}(t)$ is relative displacement between the gears along the line of action in normal plane which has a relationship with $\delta_{spur}(t)$ as shown in (7). β' is the helix angle of base circle while β is the helix angle of pitch circle. The relationship between these two angles can be expressed by (8), in which α_t is the transverse pressure angle.

$$\tan\beta' = \tan\beta\cos\alpha_t \tag{8}$$

III. Rolling Element Bearing Modelling

In the spur gear system, we can use deep groove ball bearings to support the shafts and gears. However, in the helical gear system, we need to use bearings with abilities of sustaining axial load and vibration. In our gearbox test rig, the angular contact ball bearings are used to support the gear-rotor system. Therefore, in this section we study the nonlinear characteristics of angular contact ball bearings.

We adopt the ideas proposed by N. Sawalhi and R.B. Randall [13] to establish the model of bearings in the gearbox, as shown in Fig. 3. The model introduced two extra degrees of freedom for the bearing pedestal, which can be used to study the vibration of the gearbox housing since the bearing pedestal of every bearing in the gearbox is fixed to the gearbox housing.

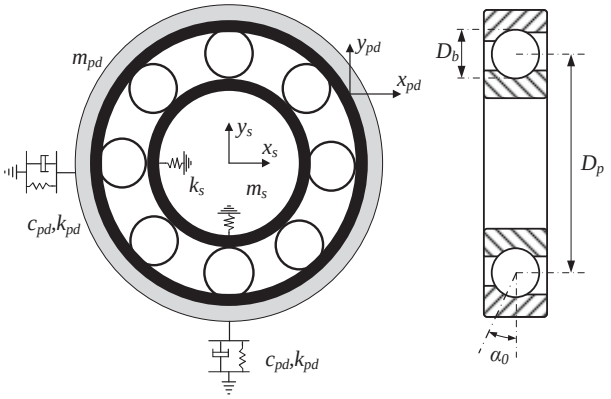

Figure 3. Angular contact ball bearing model.

There are four degrees of freedom in the above model, and the overall contact deformation for the j^{th} rolling element δ_j ($j=1,2\cdots,n_b$) is a function of the inner-race displacement relative to the outer-race in the *x*- and *y*- directions (x_s, y_s, x_{pd}, y_{pd}), the element position ϕ_j and the clearance c, where n_b is the number of rolling elements, as presented in (9).

$$\delta_j = (x_s - x_{pd})\cos\phi_j + (y_s - y_{pd})\sin\phi_j - c \tag{9}$$

$$\begin{cases} \phi_j = \dfrac{2\pi(j-1)}{n_b} + w_c t + \phi_0 \\ w_c = \dfrac{w_s}{2}(1 - \dfrac{D_b}{D_p}) \end{cases} \tag{10}$$

The element position ϕ_j is time-varying which is given as (10), in which w_c, w_s, D_b, D_p represent the speed of the cage and the shaft, the diameter of the element and the bearing pitch respectively.

For angular contact ball bearing, the normal contact pressure generated by the j^{th} ball with the raceways is decomposed into radial and axial components(f_{rj}, f_{aj}), which can be expressed by

$$\begin{cases} f_{rj} = k_b\delta_j^{1.5}\cos\alpha_0 \\ f_{aj} = k_b\delta_j^{1.5}\sin\alpha_0 \end{cases} \tag{11}$$

where k_b is the load deflection coefficient, α_0 represents the contact angle of the angular contact ball bearing.

In consideration of the fact that the contact force between the rolling elements and raceway is generated only by the circumstances of positive contact deformation, χ_j is introduced to represent the contact state of the j^{th} rolling element as

$$\chi_j = \begin{cases} 1 & \delta_j > 0 \\ 0 & \delta_j \le 0 \end{cases} \tag{12}$$

Hence, the total contact forces in the bearing decomposed into the direction of the coordinate axis, can be defined as follows

$$F_{bx} = k_b\sum_{j=1}^{n_b}(\chi_j\delta_j^{1.5}\cos\phi_j)\cos\alpha_0 \tag{13}$$

$$F_{by} = k_b\sum_{j=1}^{n_b}(\chi_j\delta_j^{1.5}\sin\phi_j)\cos\alpha_0 \tag{14}$$

IV. Gearbox Modelling

After the dynamics of helical gear pair with time-varying stiffness and support bearing with nonlinear characteristics are discussed in the above sections, we establish a lateral and torsional coupled dynamic model of a two-stage gearbox with helical gears, using the lumped parameter method. This model is based on our gearbox test rig, of which the schematic diagram is shown in Fig. 4, where ① to ⑩ are the lumped nodes in the model. The node ① defines the analyzed position of the input shaft and node ⑩ defines the counterpart of the output shaft. The node ⑤ and ⑥ are combined with each other in the gearbox test rig, so they are assumed to share the same coordinates ($x_{56}, y_{56}, \theta_{56}$). The driven load is a magnetic powder brake which provides adjustable load torque.

The mathematical model of the whole gearbox system is deduced as (15a) (15b) (15c) using the Newton's second law, which can be solved by numerical methods. The main parameters of the gearbox are provided by the manufacturer and are listed in Table I.

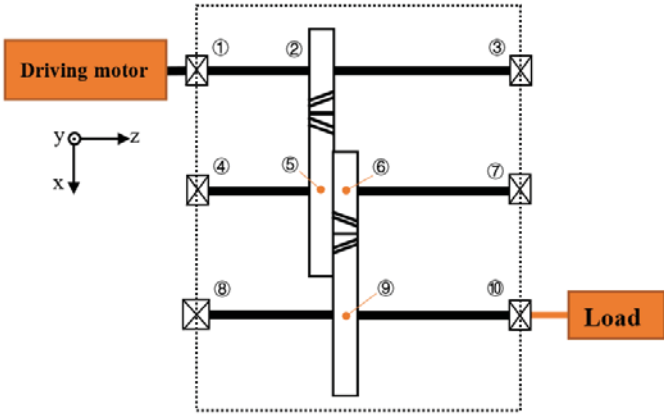

Figure 4. A top view of the two-stage gearbox model.

TABLE I. MAIN PARAMETERS OF THE GEARBOX MODEL

Part	Parameters		
	Inertia	*Stiffness*	*Damping*
Motor	$J_1 = 0.01$	/	/
Load	$J_{10} = 0.01$	/	/
Shafts	/	$k_{12} = 6.42\times10^7$	$c_{12} = 1.80\times10^5$
		$k_{23} = 5.83\times10^7$	$c_{23} = 1.48\times10^5$
		$k_{45} = 6.42\times10^7$	$c_{45} = 1.80\times10^5$
		$k_{67} = 6.15\times10^7$	$c_{67} = 1.62\times10^5$
		$k_{89} = 6.02\times10^7$	$c_{89} = 1.54\times10^5$
		$k_{910} = 6.15\times10^7$	$c_{910} = 1.62\times10^5$
		$k_{t12} = 4.5\times10^4$	$c_{t12} = 5.0\times10^5$
		$k_{t910} = 3.7\times10^4$	$c_{t910} = 4.2\times10^5$
Gears	$m_2 = 0.8$ $J_2 = 1.8\times10^{-4}$ $z_2 = 20$ β=13°		
	$m_5 = 1.5$ $J_5 = 1.3\times10^{-3}$ z_5=40 β=13°		
	$m_6 = 1.2$ $J_6 = 8.7\times10^{-4}$ z_6=25 β=13°		
	$m_9 = 3.6$ $J_9 = 2.4\times10^{-2}$ z_9=75 β=13°		
Bearings	$m_1 = 0.1$	$k_{b1} = 1.8\times10^9$	α_0=15°
	⋮	⋮	
	$m_{10} = 0.1$	$k_{b10} = 1.8\times10^9$	
Housing	$m_{1pd} = 10$	$k_{1pd} = 10^8$	$c_{1pd} = 2\times10^5$

where the units of the mass, rotating inertia, radial stiffness, torsional stiffness, radial damping coefficient and torsional damping coefficient are respectively kg, kg•m^2, N/m, Nm/rad, Ns/m, Ns/rad. J_1 and J_{10} are the rotating inertia of the driving motor and the driven load respectively, and the counterparts of the shafts and bearings are ignored. The parameters of bearings at nodes ①③④⑦⑧⑩ are considered to be the same and the parameters of the housing are similarly selected as [13].

The translational motions of the bearings and gears are governed by 15(a).

$$
\begin{cases}
m_1\ddot{x}_1 + k_{12}(x_1 - x_2) + c_{12}(\dot{x}_1 - \dot{x}_2) = -F_{bx1} \\
m_1\ddot{y}_1 + k_{12}(y_1 - y_2) + c_{12}(\dot{y}_1 - \dot{y}_2) = -F_{by1} \\
m_2\ddot{x}_2 + k_{12}(x_2 - x_1) + k_{23}(x_2 - x_3) \\
+c_{12}(\dot{x}_2 - \dot{x}_1) + c_{23}(\dot{x}_2 - \dot{x}_3) = -F_{mx2} \\
m_2\ddot{y}_2 + k_{12}(y_2 - y_1) + k_{23}(y_2 - y_3) \\
+c_{12}(\dot{y}_2 - \dot{y}_1) + c_{23}(\dot{y}_2 - \dot{y}_3) = F_{my2} - m_2 g \\
m_3\ddot{x}_3 + k_{23}(x_3 - x_2) + c_{23}(\dot{x}_3 - \dot{x}_2) = -F_{bx3} \\
m_3\ddot{y}_3 + k_{23}(y_3 - y_2) + c_{23}(\dot{y}_3 - \dot{y}_2) = -F_{by3} \\
m_4\ddot{x}_4 + k_{45}(x_4 - x_5) + c_{45}(\dot{x}_4 - \dot{x}_5) = -F_{bx4} \\
m_4\ddot{y}_4 + k_{45}(y_4 - y_5) + c_{45}(\dot{y}_4 - \dot{y}_5) = -F_{by4} \\
(m_5+m_6)\ddot{x}_{56} + k_{45}(x_{56} - x_4) + k_{67}(x_{56} - x_7) \\
+c_{45}(\dot{x}_{56} - \dot{x}_4) + c_{67}(\dot{x}_{56} - \dot{x}_7) = F_{mx2} - F_{mx6} \\
(m_5+m_6)\ddot{y}_{56} + k_{45}(y_{56} - y_4) + k_{67}(y_{56} - y_7) + c_{45}(\dot{y}_{56} - \dot{y}_4) \\
+c_{67}(\dot{y}_{56} - \dot{y}_7) = -F_{my2} - F_{my6} - (m_5 + m_6)g \\
m_7\ddot{x}_7 + k_{67}(x_7 - x_6) + c_{67}(\dot{x}_7 - \dot{x}_6) = -F_{bx7} \\
m_7\ddot{y}_7 + k_{67}(y_7 - y_6) + c_{67}(\dot{y}_7 - \dot{y}_6) = -F_{by7} \\
m_8\ddot{x}_8 + k_{89}(x_8 - x_9) + c_{89}(\dot{x}_8 - \dot{x}_9) = -F_{bx8} \\
m_8\ddot{y}_8 + k_{89}(y_8 - y_9) + c_{89}(\dot{y}_8 - \dot{y}_9) = -F_{by8} \\
m_9\ddot{x}_9 + k_{89}(x_9 - x_8) + k_{910}(x_9 - x_{10}) \\
+c_{89}(\dot{x}_9 - \dot{x}_8) + c_{910}(\dot{x}_9 - \dot{x}_{10}) = F_{mx6} \\
m_9\ddot{y}_9 + k_{89}(y_9 - y_8) + k_{910}(y_9 - y_{10}) \\
+c_{89}(\dot{y}_9 - \dot{y}_8) + c_{910}(\dot{y}_9 - \dot{y}_{10}) = F_{my6} - m_9 g \\
m_{10}\ddot{x}_{10} + k_{910}(x_{10} - x_9) + c_{910}(\dot{x}_{10} - \dot{x}_9) = -F_{bx10} \\
m_{10}\ddot{y}_{10} + k_{910}(y_{10} - y_9) + c_{910}(\dot{y}_{10} - \dot{y}_9) = -F_{bx10}
\end{cases}
\tag{15a}
$$

The translational motions of the gearbox housing are governed by 15(b).

$$
\begin{cases}
m_{1pd}\ddot{x}_{1pd} + k_{1pd}x_{1pd} + c_{1pd}\dot{x}_{1pd} = F_{bx1} \\
m_{1pd}\ddot{y}_{1pd} + k_{1pd}y_{1pd} + c_{1pd}\dot{y}_{1pd} = F_{by1} \\
\bullet\bullet\bullet
\end{cases}
\tag{15b}
$$

where the housing motions at the nodes ③/④/⑦/⑧/⑩ are the same with only changing the subscripts.

The rotational motions of the driving motor, gears and load are governed by 15(c).

$$
\begin{cases}
J_1\ddot{\theta}_1 + k_{t12}(\theta_1 - \theta_2) + c_{t12}(\dot{\theta}_1 - \dot{\theta}_2) = T_{input} \\
J_2\ddot{\theta}_2 + k_{t12}(\theta_2 - \theta_1) + c_{t12}(\dot{\theta}_2 - \dot{\theta}_1) = -F_{my2}\bullet r_2 \\
(J_5 + J_6)\ddot{\theta}_{56} = -F_{my2}\bullet r_5 + F_{my6}\bullet r_6 \\
J_9\ddot{\theta}_9 + k_{t910}(\theta_9 - \theta_{10}) + c_{t910}(\dot{\theta}_9 - \dot{\theta}_{10}) = F_{my6}\bullet r_9 \\
J_{10}\ddot{\theta}_{10} + k_{t910}(\theta_{10} - \theta_9) + c_{t910}(\dot{\theta}_{10} - \dot{\theta}_9) = -T_{output}
\end{cases}
\tag{15c}
$$

where F_{bxj}, F_{mxj} represent bearing force and gear meshing force at the j^{th} node. The radius of gears (r_2, r_5, r_6, r_9) can be calculated by the given parameters.

V. Simulations and Discussions

In this section, the differential equations of motion of (15) are solved using fourth order Runge–Kutta numerical method, and the time step in the iterative procedure is set as 10^{-4} s. Acceleration responses are calculated and analyzed in the time and frequency domain.

A. Acceleration Responses at the Input and Output Positions

In the model of this paper, we take the vibration of gearbox housing into consideration on which the acceleration data are measured. Time domain waveform and power spectrums of the simulated responses at the input and output end of the gearbox are shown as Fig. 5.

The rotation frequency of input shaft in above simulation is 30 Hz. According to the parameters provided in Table 1, two meshing frequencies can be calculated as 600Hz (of gear pair ② and ⑤) and 375Hz (of gear pair ⑥ and ⑨). As being shown in Fig. 5, the simulated result agrees well with the theoretical calculation.

It is noticed that the time domain waveform at the input and output positions are different. Moreover, we can quantitatively detect the meshing characteristic information in the spectrum, i.e., the amplitude of frequency component 375Hz in Fig. 5(c) is notable but smaller than that of the same component in Fig. 5(d), while the amplitude of 600 Hz component is larger than that of the same component in Fig. 5(d). This result agrees with the fact that the measured signal strength of the same signal at different positions is different. The closer the distance from the signal source is, the stronger the detected signal is.

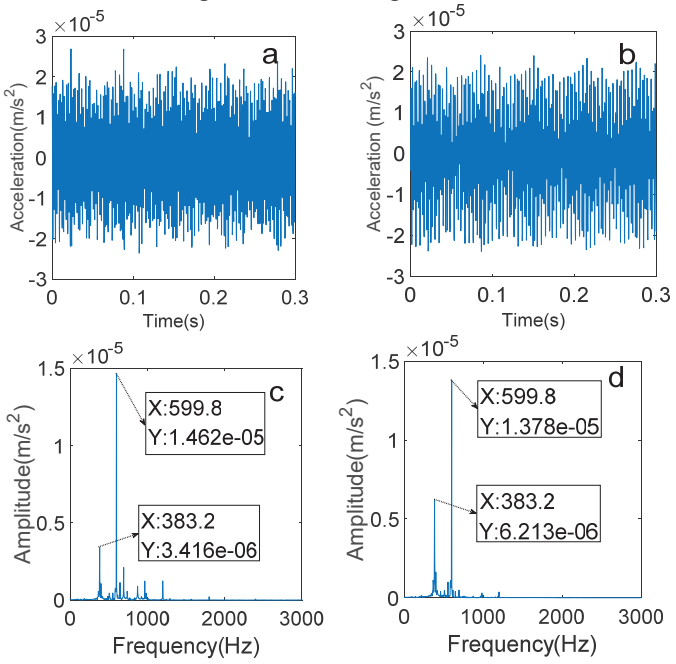

Figure 5. Simulated responses and the corresponding power spectrums at the input end (a), (c) and the output end (b), (d) of the gearbox.

B. Effect of Time-varying Stiffness on the Response

Time-varying meshing stiffness of gear pair also has significant influences on the nonlinear characteristics of gear meshing dynamics. According to (1-2) adopted in this study, the contact ratio ε_α has a positive relationship with the meshing stiffness, which is an important parameter in the design and manufacture of gears. For helical gears, the contact ratio is positively related to the helix angle. In this study, we change the contact ratio of the gear pair ② and ⑤ by directly changing the simulation parameter ε_α in (2), which can be achieved by changing the helix angle of gears in practice.

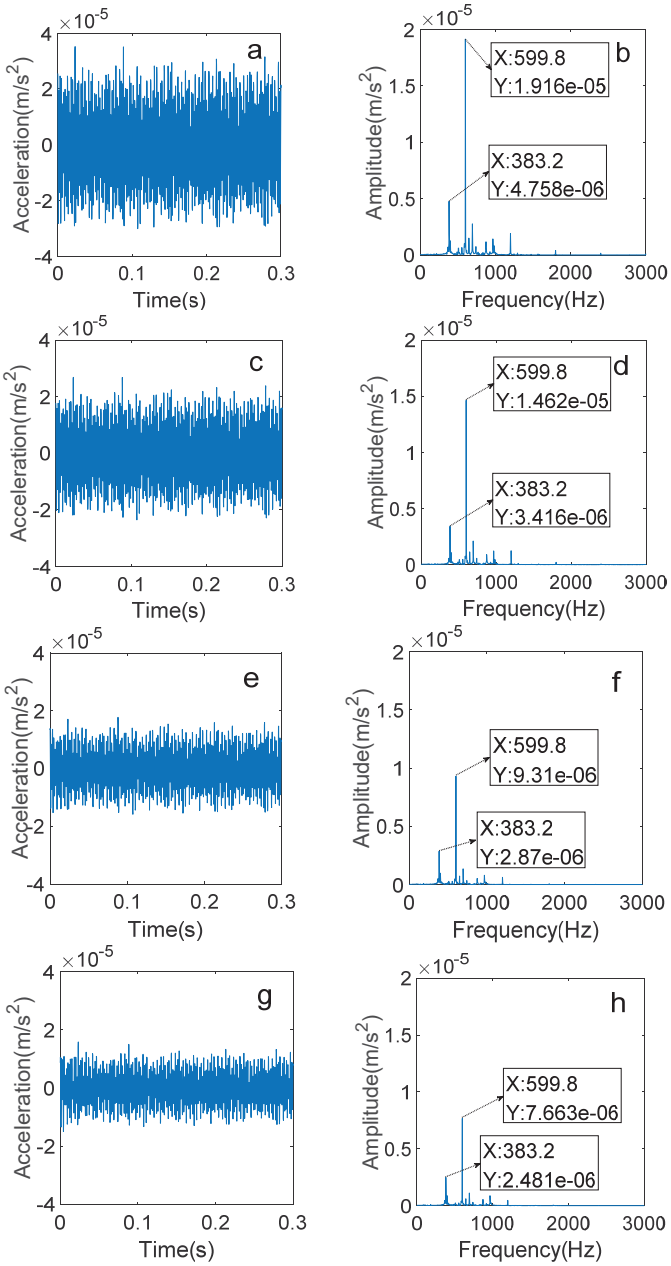

Figure 6. Simulated responses and power spectrums under the contact ratios between 2.2-2.8.

The contact ratio we studied is changed from 2.2 to 2.8 (from a to h). As shown in Fig. 6, there is an obvious decreasing trend of amplitude in both time domain and frequency domain. It is indicated that the transmission becomes more steady as the contact ratio increases which is consistent with mechanical principle. Furthermore, we calculate the energy of the different responses by the root mean square of its acceleration and the relationship between the contact ratio and the energy of the system vibration is shown as Fig. 7, which conforms to the above analysis.

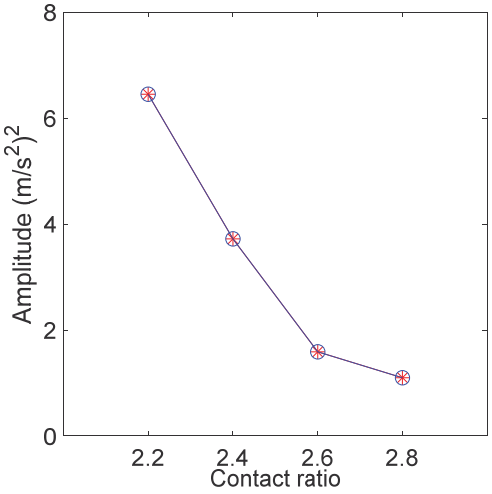

Figure 7. The comparisons of vibration energy under different contact ratios.

VI. Conclusions

In this paper, a coupling dynamic model of a two-stage gearbox test rig is established as a whole system with the consideration of time-varying meshing stiffness and non-linear characteristics of bearings. The meshing characteristics of spur gears and helical gears are comparatively studied. Moreover, vibration response at different positions of gearbox housing is simulated based on the relationship between bearing pedestal and the housing, which is usually solved by the finite element method. And the influence of time-varying meshing stiffness of gear pair on system vibration is also taken into investigation by changing the contact ratio of one gear pair.

(1) The meshing frequencies of the gearbox system are quantitatively detected in the spectrum. Besides, the amplitude of frequency component 375Hz at the input position is notable but smaller than that of the same component at the output position, while the amplitude of 600 Hz component at the input position is larger than that of the same component at the output position. This results agree with the fact that the measured signal strength of the same signal at different positions is different. The closer the distance from the signal source is, the stronger the detected signal is.

(2) It is indicated by our model that the transmission becomes steadier as the contact ratio increases. Furthermore, we calculate the energy of the different responses by the root mean square of its acceleration, and the variation patterns between the contact ratio and the vibration energy of the gearbox system further conform our conclusion.

References

[1] V. Sharma, A. Parey, "A review of gear fault diagnosis using various condition indicators." Procedia Engineering, vol. 144, 2016, pp. 253-263.

[2] D. Goyal, B. S. Pabla, and S. S. Dhami, "Condition monitoring parameters for fault diagnosis of fixed axis gearbox: a review." Archives of Computational Methods in Engineering, vol. 24(3), 2017, pp. 543-556.

[3] Z. Wan, H. Cao, and Y. Zi, "An improved time-varying mesh stiffness algorithm and dynamic modeling of gear-rotor system with tooth root crack." Engineering Failure Analysis, vol. 42, 2014, pp. 157-177.

[4] X. Liang, M. J. Zuo, and Z. Feng, "Dynamic modeling of gearbox faults: A review." Mechanical Systems and Signal Processing, vol. 98, 2018, pp. 852-876.

[5] S. Chen and J. Tang, "Nonlinear dynamic characteristics of geared rotor bearing systems with dynamic backlash and friction." Mechanism and Machine Theory, vol. 46(4), 2011,pp. 466-478.

[6] H. Ma, X. Pang, and R. Feng, "Improved time-varying mesh stiffness model of cracked spur gears." Engineering Failure Analysis, vol. 55, 2015, pp. 271-287.

[7] D. C. H. Yang, and J. Y. Lin, "Hertzian damping, tooth friction and bending elasticity in gear impact dynamics." Journal of mechanisms, transmissions, and automation in design, vol. 109, 1987, pp. 189-196.

[8] Z. Chen, and Y. Shao, "Dynamic simulation of spur gear with tooth root crack propagating along tooth width and crack depth." Engineering Failure Analysis, vol. 18, 2011, pp. 2149-2164.

[9] Y. Pandya, and A. Parey, "Simulation of crack propagation in spur gear tooth for different gear parameter and its influence on mesh stiffness." Engineering Failure Analysis, vol. 30, 2013, pp. 124-137.

[10] H. Ma, J. Zeng, and R. Feng, "Review on dynamics of cracked gear systems." Engineering Failure Analysis, vol. 55, 2015, pp. 224-245.

[11] Q. Wang, and Y. Zhang, "Coupled dynamic response of two-stage helical gear driving system." IEEE, Proceedings of 2011 International Conference on Electronic & Mechanical Engineering and Information Technology. vol. 7, 2011, pp. 3333-3336.

[12] M. Feng, H. Ma, and Z. Li, "An improved analytical method for calculating time-varying mesh stiffness of helical gears." Meccanica, vol. 53, 2018, pp. 1131-1145.

[13] N. Sawalhi, and R. B. Randall, "Simulating gear and bearing interactions in the presence of faults: Part I. The combined gear bearing dynamic model and the simulation of localised bearing faults." Mechanical Systems and Signal Processing, vol. 22, 2008, pp. 1924-1951.